



LUMINESCENCE DATING OF VOLCANOGENIC OUTBURST FLOOD SEDIMENTS FROM ASO VOLCANO AND TEPHRIC LOESS DEPOSITS, SOUTHWEST JAPAN

SUMIKO TSUKAMOTO¹, KYOKO S. KATAOKA² and YASUO MIYABUCHI³

¹*Leibniz Institute for Applied Geophysics, Stilleweg 2, Hannover D-30655, Germany*

²*Research Institute for Natural Hazards and Disaster Recovery, Niigata University, Ikarashi 2-8050, Nishi-ku, Niigata 950-2181, Japan*

³*Faculty of Education, Kumamoto University, Kurokami 2-40-1, Chuo-ku, Kumamoto 860-8555, Japan*

Received 31 January 2013

Accepted 9 September 2013

Abstract: Luminescence dating has been applied to volcanogenic outburst flood sediments (Takuma gravel bed) from Aso volcano, Japan, and tephric loess deposits overlying the gravel bed. The poly-mineral fine grains (4–11 µm) from loess deposits were measured with pulsed optically stimulated luminescence (pulsed OSL) and post-IR infrared stimulated luminescence (pIRIR) methods, whereas the Takuma gravel bed containing no quartz, was measured with IRSL and pIRIR methods using sand sized (150–200 µm) plagioclase. The loess deposits date back at least to ~50 ka by consistent IRSL, pIRIR and pulsed OSL ages from the lowermost part of the loess deposits from one section. The ages obtained from the bottom part of the other loess section are not consistent each other. However, we consider that the pIRIR age (72±6 ka) which showed negligible anomalous fading is most reliable, and regard as a preliminary minimum age of the Takuma gravel bed. The equivalent doses (D_e) for the plagioclase from the Takuma gravel bed have a narrow distribution and the weighted mean of the three samples yield an age of 89±3 ka. This age is in agreement with the last caldera-forming eruption of Aso volcano (~87 ka) and it is likely that the pIRIR signal has not been bleached before the deposition. IRSL dating without applying pIRIR using small aliquots was also conducted, however, the IRSL signal shows no clear evidence of an additional bleaching during the event of outburst flood from the caldera lake.

Keywords: IRSL, post-IR IRSL, tephric loess, Takuma gravel bed, Aso volcano, volcanogenic outburst flood.

1. INTRODUCTION

Aso volcano is one of the largest caldera volcanoes in Japan and its caldera forming eruptions provided four large-volume ignimbrites namely Aso-1, -2, -3 and -4 in the past ca. 270 ka (Ono *et al.*, 1977; Machida and Arai,

2003). It has been suggested that a caldera lake was once formed and then drained, after the Aso-4 eruption at ~87 ka (Aoki, 2008), according to the existence of lake sediments in the caldera (Watanabe, 1998; Kataoka and Miyabuchi, 2011). To the west of the caldera rim, a large-scale volcaniclastic apron is distributed along the Shira River. The apron sediments (Takuma gravel bed) directly overlie the Aso-4 pyroclastic flow deposits and the Aso-4 lahar deposits, indicating that the gravel bed was formed

Corresponding author: S. Tsukamoto
e-mail: sumiko.tsukamoto@liag-hannover.de

after the eruption of Aso-4. The Takuma gravel bed is composed of poorly sorted pebble and cobble with sandy matrix, and occasionally contains large boulders up to a few metres in diameter. The present Shira River does not have the capacity to transport such boulder rich sediments, and therefore the sediment is presumably the result of a gigantic outburst flood from the caldera lake (Kataoka and Miyabuchi, 2011).

Volcanogenic large-scale flood sediments which are associated with caldera lake outburst or failure of volcanically dammed lake have been found in many places, e.g. Numazawa and Towada volcanoes, Japan (Kataoka *et al.*, 2008; Kataoka, 2011), Aniakachak volcano, Alaska (Waythomas *et al.*, 1996), Laacher See volcano, Germany (Park and Schmincke, 1997) and Taupo volcanic zone, New Zealand (Manville *et al.*, 1999). In this study, we apply luminescence dating for the first time to volcanogenic outburst flood sediments from Aso volcano (Takuma gravel bed) and also to the overlying tephric loess deposits to constrain the age of the possible intra-caldera lake outburst event.

2. STUDY AREA AND SAMPLES

Partly terraced volcaniclastic apron surface in west of Aso caldera has been subdivided into the Takuma and Hotakubo surfaces (Watanabe *et al.*, 1995). The higher Takuma surface (30–70 m a.s.l.) is a depositional surface of Takuma gravel bed and lower Hotakubo surface (~20 m a.s.l.) is presumably an erosional surface (fill-strath terrace). The latter surface is covered by 1.5–2 m tephric loess, which contains two horizons of volcanic glasses concentration derived from two widespread tephra (Kikai-Akahoya tephra, 6.3 ka and Aira-Tanzawa tephra, 29 ka) at ~0.3 m and 0.8–1.2 m from the surface, respectively (Watanabe *et al.* 1995). According to the thickness of the loess and the stratigraphic horizons of

widespread tephra in the loess sequence, Watanabe *et al.* (1995) assumed that the Hotakubo surface was formed at 40–50 ka. Therefore, the age of the Takuma surface is older than 40–50 ka and younger than Aso-4 (~87 ka).

Samples for luminescence dating were taken from two outcrops in the area of the National Agriculture Research Center for Kyushu Okinawa Region which is located about 25 km from the west of the breached caldera rim, close to the lower edge of the Takuma surface (Fig. 1). These outcrops are located at the wall of two trenches which were made for collecting surface water in case of heavy rain, in order to protect the area from flooding. The Takuma gravel bed and tephric loess are nicely exposed on the walls. Altogether, ten samples for luminescence dating were taken from Takuma gravel bed and tephric loess overlying the gravel bed. At Site 1 (“Mizuana-4”, i.e., trench no. 4: 32° 52' 30.3" N / 130° 44' 38.0" E), ~3 m thick tephric loess covers the Takuma gravel bed (Fig. 2a). The upper 1 m of the tephric loess comprises so-called Kuroboku soil (black andisols) which is a typical dark coloured humic soil found near active volcanoes in Japan. The Takuma gravel bed here is more than 3 m thick, and shows crude parallel to low-angle cross stratifications which suggest a rapid deposition by a hyperconcentrated flow process (Kataoka and Miyabuchi, 2011). Four samples from tephric loess (AS-TL-1, -2, -3, 4) and two samples from the Takuma gravel bed (AS-TGB-1 and -2) were collected from this site.

Site 2 (“Mizuana-2”, trench no. 2: 32° 52' 55.4" N / 130° 44' 40.8" E) is located ~700 m northeast of Site 1. At this site, about 4 m of diffusely stratified Takuma gravel bed including metre-sized boulders and ~2.5 m thick tephric loess are exposed (Fig. 2b). Three samples from tephric loess (AS-TL-7, -8, and -9) and one sample (AS-TGB-4) from the uppermost part of the Takuma gravel bed were taken for luminescence dating from Site 2.

3. SAMPLE PREPARATION AND LUMINESCENCE EQUIPMENTS

The Takuma gravel bed comprises volcaniclastic materials which were derived mainly from the Aso 1–4 ignimbrites and pre-Aso volcanic rocks (Ono and Watanabe, 1985) entrained by the watery flow. An X-ray diffraction analysis of samples from the gravel bed (AS-TGB-1, 2, and 4) indicates that these samples contain plagioclase, clino- and ortho-pyroxenes, magnetite, and hornblende, as well as volcanic glass shards. These minerals reflect the typical dacitic composition of Aso volcano. The sample TGB-4, taken close to the upper surface of TGB, also contains short-range order minerals (imogolite and/or allophane) which are commonly developed in volcanic soils in Japan (Wada, 1987). These samples do not yield quartz and K-feldspar which are normally used as luminescence dosimeters. Therefore, a sand-sized (150–200 µm) plagioclase rich fraction was separated from heavy minerals using a sodium polytungstate solu-

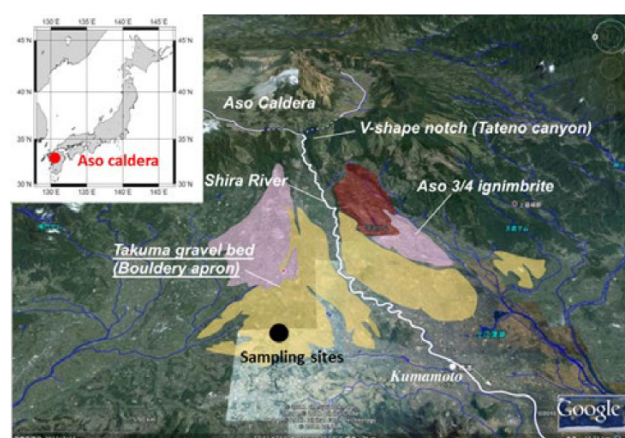


Fig. 1. Overview of Aso caldera and the distribution of volcanic apron (modified from Kataoka and Miyabuchi, 2011). Location of sampling sites is shown in black circle. Inset shows a map showing the location of Aso caldera.

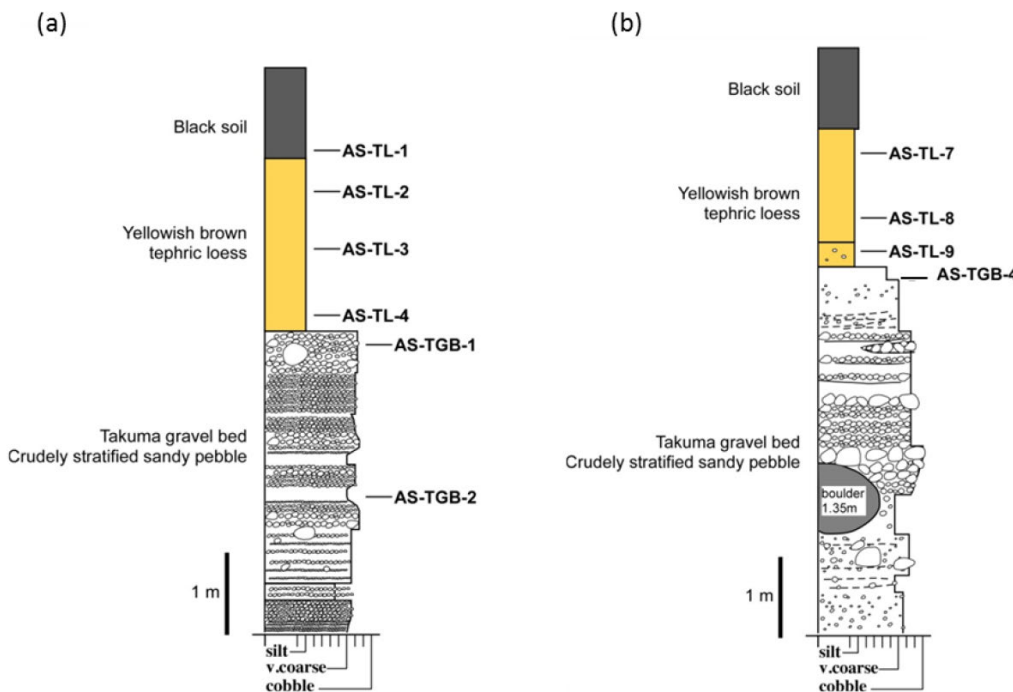


Fig. 2. Graphic sedimentary logs at (a) Site 1, so-called “Mizuana-4” and (b) Site 2, “Mizuana-2”. The positions of luminescence samples are shown.

tion ($d < 2.68$) for AS-TGB-1, -2, and -4, after treating with hydrochloric acid (HCl), sodium oxalate ($\text{Na}_2\text{C}_2\text{O}_4$) and hydrogen peroxide (H_2O_2). For tephric loess samples, polymineral fine grains (4–11 μm) were prepared using a standard procedure following Frechen *et al.* (1996). The sand sized grains were mounted on stainless steel discs using silicon spray for luminescence measurements using either 6 or 2.5 mm mask size. Polymineral fine grains were settled on aluminium discs using acetone or distilled water.

All luminescence measurements were carried out by an automated reader (Risø TL/OSL-20) equipped with blue and IR LEDs for optical stimulation and a $^{90}\text{Sr}/^{90}\text{Y}$ beta source (1.48 GBq) for irradiation. Infrared stimulated luminescence (IRSL) signals were detected through a combination of 2 mm thick Schott BG-39 and 4 mm thick Corning 7-59 filters (detection: 320–460 nm). Pulsed optically stimulated luminescence (OSL) signals were measured with 50 μs on- and off-times, and only the off-time signal starting at 2.5 μs , after the pulses switched off, was recorded. A 7.5 mm HOYA U-340 (280–360 nm) was used as a detection filter for pulsed OSL measurements.

4. LUMINESCENCE DATING

Dose rate

High-resolution gamma spectrometry with an N-type coaxial detector was used for the estimation of external dose rates. For each sample, homogenised material of 50 g was used for gamma spectrometry measurements. The activities of ^{234}Th , ^{214}Bi , ^{214}Pb (for U), ^{228}Ac , ^{208}Tl ,

^{212}Pb (for Th) and ^{40}K were converted into U, Th and K concentrations to calculate annual dose rate using the conversion factors by Guérin *et al.* (2011). Natural water contents (water/dry sediment) were measured for all samples soon after sampling, however, as mentioned above, the studied sections are the walls of water reservoirs to collect surface water, and some of the measured contents were very high (up to 104% and 37% for tephric loess and the Takuma gravel bed, respectively). These measured water contents are probably much higher than the water contents for the samples averaged over the burial time. Therefore, we used a water content of 15% (assuming an uncertainty of $\pm 10\%$) obtained from the Takuma gravel bed outside the National Agriculture Research Center to calculate dose rates for all Takuma gravel bed samples. A water content of 60% ($\pm 20\%$) was used for tephric loess samples, which was measured from a wall from another trench wall in the research centre under a relatively dry condition. Alpha efficiencies (a -values) of 0.09 ± 0.02 , 0.11 ± 0.02 , and 0.035 ± 0.03 were used for IRSL, post-IR IRSL, and pulsed OSL signals, respectively (Kreuzer *et al.*, submitted; Lai *et al.*, 2008). The cosmic dose rate was calculated according to the altitude and geomagnetic latitude from the sampling sites, and the sampling depth from the surface based on Prescott and Hutton (1994). The total dose rates are summarised in Table 1.

Post-IR IRSL (pIRIR) and pulsed OSL dating of tephric loess

For dating of tephric loess, the luminescence from polymineral fine grains were measured using two differ-

ent methods, i.e. post-IR IRSL (pIRIR) to measure feldspar luminescence and pulsed OSL to measure quartz signal. Tephric loess in Japan has been considered to be a mixture of air-fall tephra from small-scale volcanic eruptions, loess from the Asian continent, and local dusts from adjacent non-vegetated areas (Suzuki, 1995; Tsukamoto *et al.*, 2003). It has been reported that OSL dating of fine grain quartz from Japanese tephric loess is often problematic (Tsukamoto *et al.*, 2003; Watanuki *et al.*, 2005), because volcanic quartz has undesirable OSL characteristics (Tsukamoto *et al.*, 2007). Such problem does not exist when the pIRIR protocol is applied (Thiel *et al.*, 2011b). Since the study area does not have any source of quartz, it is expected that the pulsed OSL from quartz works well only if there is enough amounts of aeolian loess from the Asian continent.

For pulsed OSL luminescence signals are stimulated by pulsed LED light instead of normal continuous wave stimulation (Denby *et al.*, 2006; Lapp *et al.*, 2009). The lifetime of feldspar OSL signal is much shorter than that of quartz OSL, i.e. the feldspar signal decays quickly after the LED pulses switch off, and therefore when a luminescence signal from a mixture of quartz and feldspar is measured, the off-time signal should be dominated by quartz OSL.

IRSL and pIRIR

A single aliquot regenerative dose (SAR) protocol using a post-IR IRSL signal at 290°C (pIRIR₂₉₀) after pre-heated the samples at 320 °C for 60 s and bleached with IR at 50°C for 100 s (**Table 2**) was applied for D_e measurements. This protocol, first introduced by Thiel *et al.* (2011a), has been successfully applied to both poly-mineral fine grains and K-feldspar without a fading correction (e.g. Buylaert *et al.*, 2012). The pIRIR₂₉₀ signal was measured for 200 s, but the IR LEDs were switched on 5 s after the temperature reached to 290°C, in order to monitor thermally stimulated signal if any. No significant thermal signal was detected. The integrated intensity of the initial 5 s minus the last 25 s signal as background was used for the D_e calculation. The D_e values from the IRSL signal (IR₅₀) prior to pIRIR₂₉₀ were also calculated using the integrated intensity of the initial 4 s signal minus the last 10 s. The second regenerative dose (74 Gy) cycle was repeated once again after measuring the highest regenerative dose cycle, and the recycling ratio was calculated for all measured aliquots. The D_e values were calculated only from the aliquots which gave the recycling ratio within 10% from the unity.

A dose recovery test was conducted after bleaching aliquots using a solar simulator (SOL2) for 4 hours and giving a beta dose of 123 Gy, in order to test if the ap-

Table 1. Summary of dose rate.

Sample	U (ppm)	Th (ppm)	K (%)	Cosmic dose rate (Gy/ka)	Dose rate for IRSL (Gy/ka)	Dose rate for pIRIR (Gy/ka)	Dose rate for pulsed OSL (Gy/ka)
AS-TL-1	3.96 ± 0.04	15.0 ± 0.11	1.25 ± 0.02	0.19 ± 0.02	2.93 ± 0.21	3.11 ± 0.21	2.42 ± 0.17
AS-TL-2	4.24 ± 0.04	17.2 ± 0.11	1.37 ± 0.02	0.17 ± 0.02	3.21 ± 0.22	3.42 ± 0.22	2.65 ± 0.17
AS-TL-3	3.77 ± 0.04	15.0 ± 0.10	1.23 ± 0.02	0.16 ± 0.02	2.85 ± 0.21	3.03 ± 0.21	2.35 ± 0.17
AS-TL-4	3.27 ± 0.04	12.4 ± 0.09	1.22 ± 0.02	0.14 ± 0.01	2.52 ± 0.2	2.67 ± 0.20	2.10 ± 0.17
AS-TL-7	4.16 ± 0.03	16.6 ± 0.08	1.36 ± 0.01	0.17 ± 0.02	3.14 ± 0.22	3.34 ± 0.22	2.59 ± 0.17
AS-TL-8	3.62 ± 0.04	13.3 ± 0.09	0.95 ± 0.02	0.16 ± 0.02	2.52 ± 0.2	2.69 ± 0.20	2.07 ± 0.17
AS-TL-9	2.57 ± 0.04	10.1 ± 0.08	1.07 ± 0.02	0.16 ± 0.02	2.11 ± 0.19	2.24 ± 0.19	1.78 ± 0.16
AS-TGB-1	2.25 ± 0.04	9.30 ± 0.10	1.68 ± 0.03	0.13 ± 0.01	2.59 ± 0.17	2.62 ± 0.17	
AS-TGB-2	2.45 ± 0.03	9.58 ± 0.09	1.74 ± 0.02	0.11 ± 0.01	2.68 ± 0.17	2.71 ± 0.17	
AS-TGB-4	2.40 ± 0.04	9.24 ± 0.10	1.37 ± 0.02	0.15 ± 0.01	2.38 ± 0.17	2.41 ± 0.17	

Table 2. IRSL and post-IR IRSL protocols used in this study.

a	Polymineral pIRIR ₂₉₀		b	Polymineral pulsed OSL		c	Plagioclase pIRIR ₃₀₀		d	Plagioclase IR ₅₀	
Step	Treatment	Observed	Step	Treatment	Observed	Step	Treatment	Observed	Step	Treatment	Observed
1	Dose		1	Dose		1	Dose		1	Dose	
2	Preheat 320°C 60 s		2	Preheat 220°C 10 s		2	Preheat 340°C 60 s		2	Preheat 280°C 60 s	
3	IRSL 50°C 100 s	L _x	3	IRSL 125°C 200 s		3	IRSL 50°C 100 s	L _x	3	IRSL 50°C 200 s	L _x
4	pIRIR 290°C 200 s	L _x	4	pulsed OSL (50 µs on/off) 125°C 200 s	L _x	4	pIRIR 300°C 400 s	L _x	4	Test Dose	
5	Test Dose		5	Test Dose		5	Test Dose		5	Preheat 280°C 60 s	
6	Preheat 320°C 60 s		6	Cutheat 200°C 0 s		6	Preheat 340°C 60 s		6	IRSL 50°C 200 s	T _x
7	IRSL 50°C 100 s	T _x	7	IRSL 125°C 200 s		7	IRSL 50°C 100 s	T _x			
8	pIRIR 290°C 200 s	T _x	8	pulsed OSL (50 µs on/off) 125°C 200 s	T _x	8	pIRIR 300°C 400 s	T _x			
9	Back to 1					9	Back to 1				

plied protocol can recover the known given dose. The residual dose after the 4 hour bleaching was also measured (**Table 3**) and subtracted from the recovered dose when the dose recovery ratio was calculated. However, the residual doses were not subtracted from the D_e values. Sohbati *et al.* (2012) and Buylaert *et al.* (2012) reported an increase in measured residual doses with D_e values, after a 4 h SOL2 bleaching. They interpret that the SOL2 bleach could not reproduce the sunlight bleaching before burial. The residual doses for the pIRIR₂₉₀ signal obtained from our loess samples are plotted against D_e values (**Fig. 3**). There is a clear increase of the residual dose with D_e value, although the two bottom samples (AS-TL4 and -8) have a different trend. The fitted line using 5 data points excluding AS-TL4 and -8 goes close to the origin, suggesting that there was no residual before burial.

The dose recovery ratio was satisfactory ($\pm 10\%$ from the unity) for most of the samples for the pIRIR₂₉₀ signal except the two bottom samples from each section which yielded lower dose recovery ratios, ~ 0.8 (AS-TL-4, and -8; **Table 3**). The mean dose recovery ratio for pIRIR₂₉₀ is

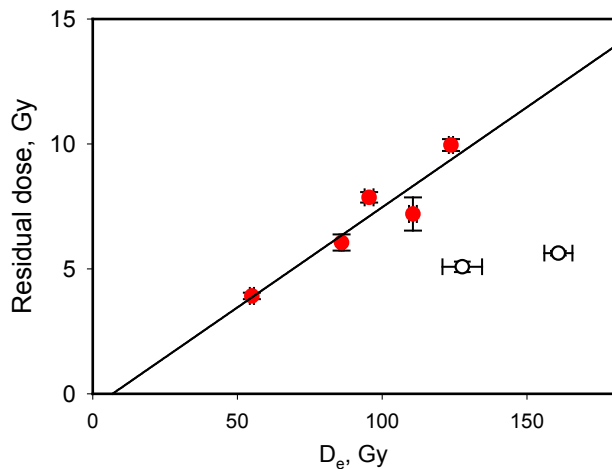


Fig. 3. Relationship between D_e and residual dose for IR₅₀ and pIRIR₂₉₀ signals from tephric loess samples.

Table 3. Equivalent dose and ages.

Sample	Signal	D_e (Gy)*	σ_{OD} (%)	Residual dose (Gy)	Dose recovery ratio	g-value (%/decade)	Fading uncorrected age (ka)	Fading corrected age (ka)
AS-TL-1	IR ₅₀ (pIR)	44.3 \pm 0.8		1.5 \pm 0.1	0.97 \pm 0.03	1.6 \pm 0.3	15.1 \pm 1.1	17.3 \pm 1.4
	pIRIR ₂₉₀	55.0 \pm 0.7		3.9 \pm 0.1	0.98 \pm 0.02	1.0 \pm 0.1	17.7 \pm 1.2	
	pulsed OSL	46.4 \pm 1.3			0.90 \pm 0.01	1.0 \pm 0.2	19.1 \pm 1.4	
AS-TL-2	IR ₅₀ (pIR)	59.4 \pm 1.5		2.7 \pm 0.5	0.79 \pm 0.05	1.6 \pm 0.4	18.5 \pm 1.3	21.2 \pm 1.6
	pIRIR ₂₉₀	95.5 \pm 1.5		7.9 \pm 0.2	0.98 \pm 0.02	1.0 \pm 0.2	27.9 \pm 1.9	
	pulsed OSL	68.7 \pm 4.7			1.00 \pm 0.03	1.0 \pm 0.6	25.8 \pm 2.4	
AS-TL-3	IR ₅₀ (pIR)	72.8 \pm 2.1		3.9 \pm 0.3	0.80 \pm 0.08	1.4 \pm 0.3	25.6 \pm 2.0	29.4 \pm 2.4
	pIRIR ₂₉₀	124 \pm 1		10.0 \pm 0.2	1.09 \pm 0.05	1.3 \pm 0.2	40.9 \pm 2.8	
	pulsed OSL	109 \pm 3			1.04 \pm 0.01	-0.2 \pm 1.6	46.0 \pm 3.5	
AS-TL-4	IR ₅₀ (pIR)	95.0 \pm 1.9		2.1 \pm 0.2	0.73 \pm 0.07	1.9 \pm 0.7	37.8 \pm 3.0	45.0 \pm 4.7
	pIRIR ₂₉₀	128 \pm 7		5.1 \pm 0.2	0.78 \pm 0.05	0.4 \pm 0.2	47.8 \pm 4.4	
	pulsed OSL	75.3 \pm 6.3			0.90 \pm 0.14	3.9 \pm 1.5	35.9 \pm 4.1	50.3 \pm 9.1
AS-TL-7	IR ₅₀ (pIR)	53.8 \pm 0.4		1.9 \pm 0.3	0.82 \pm 0.01	1.8 \pm 0.4	17.1 \pm 1.2	20.0 \pm 1.6
	pIRIR ₂₉₀	85.9 \pm 0.7		6.1 \pm 0.3	1.00 \pm 0.02	0.8 \pm 0.1	25.7 \pm 1.7	
	pulsed OSL	45.8 \pm 1.6			0.91 \pm 0.01	0.9 \pm 0.4	17.6 \pm 1.3	
AS-TL-8	IR ₅₀ (pIR)	71.9 \pm 2.5		2.7 \pm 1.6	0.91 \pm 0.21	1.7 \pm 0.5	28.5 \pm 2.5	33.0 \pm 3.2
	pIRIR ₂₉₀	111 \pm 1		7.2 \pm 0.7	1.00 \pm 0.10	1.0 \pm 0.4	41.1 \pm 3.1	
	pulsed OSL	84.1 \pm 11.2			1.04 \pm 0.05	2.0 \pm 1.5	40.6 \pm 6.3	47.2 \pm 8.9
AS-TL-9	IR ₅₀ (pIR)	149 \pm 7		2.2 \pm 0.7	0.84 \pm 0.06	2.1 \pm 0.4	70.5 \pm 6.9	86.8 \pm 11.1
	pIRIR ₂₉₀	161 \pm 5		5.6 \pm 0.1	0.79 \pm 0.03	0.5 \pm 0.2	71.9 \pm 6.3	
	pulsed OSL	72.0 \pm 6.9			0.92 \pm 0.01	1.6 \pm 0.3	40.5 \pm 5.4	46.2 \pm 6.3
AS-TGB-1	IR ₅₀ (pIR)	177 \pm 12	29	4.0 \pm 0.9	1.32 \pm 0.14		68.3 \pm 6.5	
	pIRIR ₃₀₀	235 \pm 10	17	8.1 \pm 1.3	0.94 \pm 0.09	0.7 \pm 0.7	89.9 \pm 7.1	
	IR ₅₀	139 \pm 6	28		0.95 \pm 0.04		53.6 \pm 4.2	
AS-TGB-2	IR ₅₀ (pIR)	181 \pm 10	23	2.0 \pm 0.4	1.03 \pm 0.15		67.5 \pm 5.7	
	pIRIR ₃₀₀	221 \pm 8	15	6.9 \pm 0.8	0.87 \pm 0.03	0.4 \pm 0.3	81.7 \pm 6.1	
	IR ₅₀	130 \pm 6	30		0.93 \pm 0.04		48.6 \pm 3.8	
AS-TGB-4	IR ₅₀ (pIR)	223 \pm 9	16	3.7 \pm 1.0	1.09 \pm 0.16		93.6 \pm 7.8	
	pIRIR ₃₀₀	241 \pm 7	10	7.3 \pm 0.8	0.87 \pm 0.07	0.7 \pm 0.4	101 \pm 8	
	IR ₅₀	158 \pm 6	22		0.94 \pm 0.04		66.5 \pm 5.4	

* D_e values were calculated using arithmetic mean for AS-TL-1-9 and the Central Age Model for AS-TGB-1, 2, and 4.

Only the aliquots with a recycling ratio of $\pm 10\%$ from the unity were used for the D_e calculation.

0.95 ± 0.04 , but tended to underestimate for the IR₅₀ signal (0.81 ± 0.03 ; **Table 3**). The IR₅₀ and pIRIR₂₉₀ D_e values were measured using 6 aliquots for each sample and ranged from 44 to 149 Gy for IR₅₀ and 55 to 161 Gy for pIRIR₂₉₀.

An anomalous fading test was conducted using a procedure following Auclair *et al.* (2003) by repeatedly measuring regenerated (L_x) and test dose (T_x) signals with various durations of delay (0.2–50 hours) between the irradiation and the L_x measurements. The fading rate (g-value) for IR₅₀ is between 1.4 and 2.1%/decade and that for pIRIR₂₉₀ signals is between 0.4 and 1.3%/decade, confirming that the fading is negligible for pIRIR₂₉₀ signal and therefore, there is no need for a fading correction (Buylaert *et al.*, 2012). Such small fading rate of < 1.3%/decade has been almost always measured from the pIRIR₂₉₀ signal, which has been considered as a laboratory artefact (Thiel *et al.*, 2011a, 2011b; Buylaert *et al.*, 2012). The resulting pIRIR₂₉₀ ages for tephric loess are ranging from 18 to 44 ka for Site 1 and from 18 to 72 ka for Site 2 (**Table 3**). The IR₅₀ ages were corrected for anomalous fading using the method of Huntley and Lamothe (2001), and the fading corrected ages are still underestimating the pIRIR₂₉₀ ages for 4 samples (out of 7). This could be because of the low dose recovery ratio of IR₅₀ signal (**Table 3**), and therefore we conclude that our IR₅₀ ages from the tephric loess measured as a part of the pIRIR₂₉₀ protocol are less reliable than the pIRIR₂₉₀ ages.

Pulsed OSL

Pulsed OSL D_e values were measured by pulsed blue LED stimulation (50 µs on, 50 µs off) for 200 s using a preheat of 220°C for 10 s and a cut heat of 200°C (**Table 2**). An IR bleaching for 200 s was always inserted before the pulsed OSL stimulations to bleach feldspar OSL signal as much as possible before stimulating with blue LEDs. Although pulsed OSL is a powerful method to obtain quartz dominated OSL signals from a mixed quartz/feldspar sample, its effectiveness depends on the contribution of quartz OSL in the bulk OSL signal. If there is too little quartz in polymineral fine grain samples, the pulsed OSL can be still dominated by feldspar OSL signal. Interestingly, the intensity of pulsed OSL signal (measured as a test dose OSL after 48 Gy beta irradiation) decreased significantly with depth for both Site 1 and 2. **Fig. 4** shows the test dose OSL signals for 4 samples from Site 1. This suggests that the amount of quartz in the loess have been increased with time. Such a difference in the luminescence intensity was not observed in the IRSL and pIRIR signals.

A dose recovery test was done by bleaching natural OSL signal using blue LEDs for 500 s twice then giving a dose of 72 Gy as a surrogate of natural dose. A fading test was also conducted with delays between 0.2 and 26 hours, because it is possible that not all pulsed OSL originates from quartz, as mentioned above.

The dose recovery ratios for all samples are within the acceptable range (0.9–1.1, **Table 3**). The fading rates are negligible for samples (AS-TL-1, 2, 3, and 7: 0–1.0%/decade). However, the g-values are larger for the other three samples whose signals are dim (AS-TL-4, 8, and 9: 1.6–3.9%/decade), and the ages of these samples were corrected for fading using the method of Huntley and Lamothe (2001). The final pulsed OSL ages (fading corrected or uncorrected, depending on the fading rate) are listed in **Table 3**.

Comparison between IRSL, pIRIR and pulsed OSL ages of tephric loess

The luminescence characteristics of different signals suggests that all pIRIR₂₉₀ ages and the pulsed OSL ages for 4 samples (AS-TL-1, 2, 3, 7), whose signals showed negligible fading, are more reliable than all IR₅₀ ages and rest of the pulsed OSL ages which needed fading corrections. The pIRIR₂₉₀ and pulsed OSL signals have good dose recovery ratios for most of the samples whereas IR₅₀ dose recovery ratio underestimates from the unity. Therefore, we exclude the IR₅₀ ages (as measured part of the pIRIR₂₉₀ protocol) from our interpretation.

The difference in the characteristics of pulsed OSL signal between the samples presumably reflects the change in the dominant source of loess. The pulsed OSL signal from AS-TL-1, 2, 7 are in particular, much brighter than the other samples, probably because the samples contain more aeolian loess component from the Asian continent, rather than the local origin.

Fig. 5 shows IR₅₀, pIRIR₂₉₀ and pulsed OSL ages for all tephric loess samples. All pIRIR₂₉₀ and pulsed OSL ages from 4 samples from Site 1 are consistent within 1- σ uncertainty, ranging from ~18–19 ka up to ~48–50 ka. However, the ages from Site 2 show larger scatter in ages obtained from different methods. For AS-TL-8 the pIRIR₂₉₀ and pulsed OSL ages agreed and yielded similar ages (41–47 ka). However, the pIRIR₂₉₀ and pulsed OSL

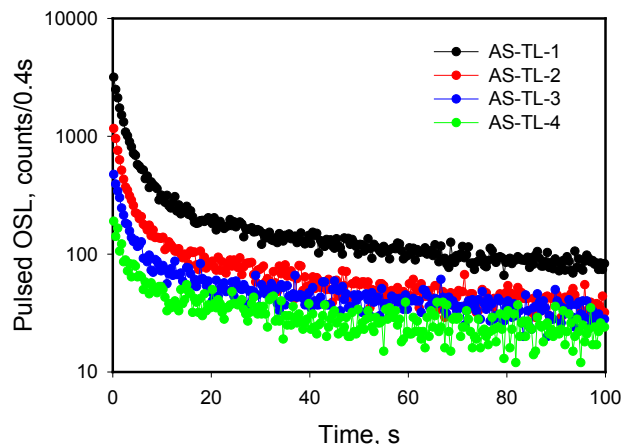


Fig. 4. Pulsed OSL decay curves for AS-TL-1–4 from Site 1.

ages are significantly different for the lowermost sample, AS-TL-9 (72 ± 6 ka for pIRIR₂₉₀, 46 ± 6 ka for pulsed OSL after fading correction). The pulsed OSL signal from this sample was very dim, suggesting the sample contains very little amount of quartz, and therefore, pulsed OSL is not a suitable method for this sample. The pIRIR₂₉₀ age of 72 ± 6 ka should be more reliable, despite the lower dose recovery ratio (0.79 ± 0.03). We therefore regard 72 ± 6 ka as a preliminary minimum age of Takuma gravel bed.

IRSL and post-IR IRSL dating of Takuma gravel bed

Plagioclase originated from Aso volcano is relatively Ca-rich (between An₃₇ and An₈₆, according to Hunter, 1998). This type of feldspar has been only limitedly applied to luminescence dating for estimating ages of volcanic eruption (e.g. Tsukamoto *et al.*, 2010; 2011), but has not yet been used for dating sediments containing volcaniclastic materials settled by water processes. From the luminescence studies of basalt including Ca-rich plagioclase, very high fading rates of up to $\sim 30\%/\text{decade}$ were reported by Mortheikai *et al.* (2008) and Tsukamoto and Duller (2008).

Since minimising anomalous fading is a critical issue in dating volcanic plagioclase, a post-IR IRSL protocol with a preheat at 340°C for 60 s and pIRIR stimulation temperature of 300°C (400 s) was selected for Takuma gravel bed samples (Table 2). The higher preheat temperature reduces the number of possible recombination centres, and therefore reduces the chance of anomalous fading (Jain and Ankjærgaard, 2011). Fig. 6 shows IR₅₀ and pIRIR₃₀₀ decay curves and dose response curves for an aliquot of AS-TGB-1. The IR₅₀ signal is very dim compared to the pIRIR₃₀₀ signal after applying the 340°C preheat. A dose recovery and a fading test were also conducted for all three samples in the same manner as with the tephric loess samples. The integrated intensity of the first 4 s minus last 10 s was used for the IR₅₀ signal,

and the intensity of the initial 20 s minus last 80 s was used for the pIRIR₃₀₀ signal. The dose recovery ratios after subtracting the residual doses are ranging from 1.03 ± 0.15 to 1.32 ± 0.14 for the IR₅₀ signal and from 0.87 ± 0.03 to 0.94 ± 0.09 for the pIRIR₃₀₀ signal. The measured anomalous fading rates were negligible for the pIRIR₃₀₀ signal; 0.68 ± 0.72 , 0.44 ± 0.32 , and $0.69 \pm 0.42\%/\text{decade}$ for AS-TGB-1, -2, and -4, indicating that there is no need for a fading correction. However, there was a significant scatter in the fading rates between aliquots for the IR₅₀ signal. Some aliquots showed clear increase with the delay time after irradiation. Thiel *et al.* (2011b) also reported minus fading rates from some of their samples from Japanese tephric loess; the reason has not been understood. Therefore we did not apply a fading correction for the IR₅₀ ages from the Takuma gravel bed. The D_e values were measured with using 6 mm aliquots, and were calculated with the Central Age Model (CAM) by Galbraith *et al.* (1999). The pIRIR₃₀₀ D_e values have tight and normal dose distributions of the pIRIR D_e val-

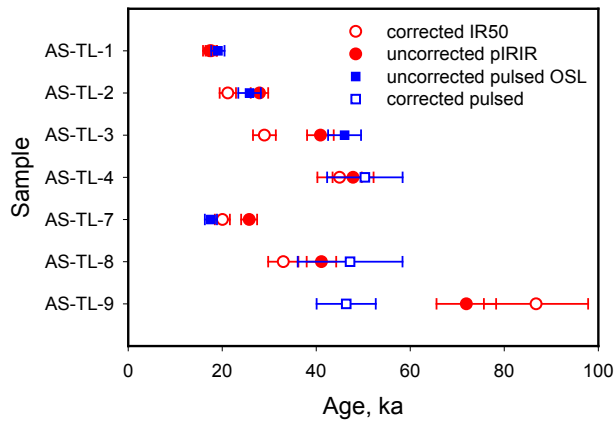


Fig. 5. Summary of IR₅₀, pIRIR₂₉₀ and pulsed OSL ages for all tephric loess samples.

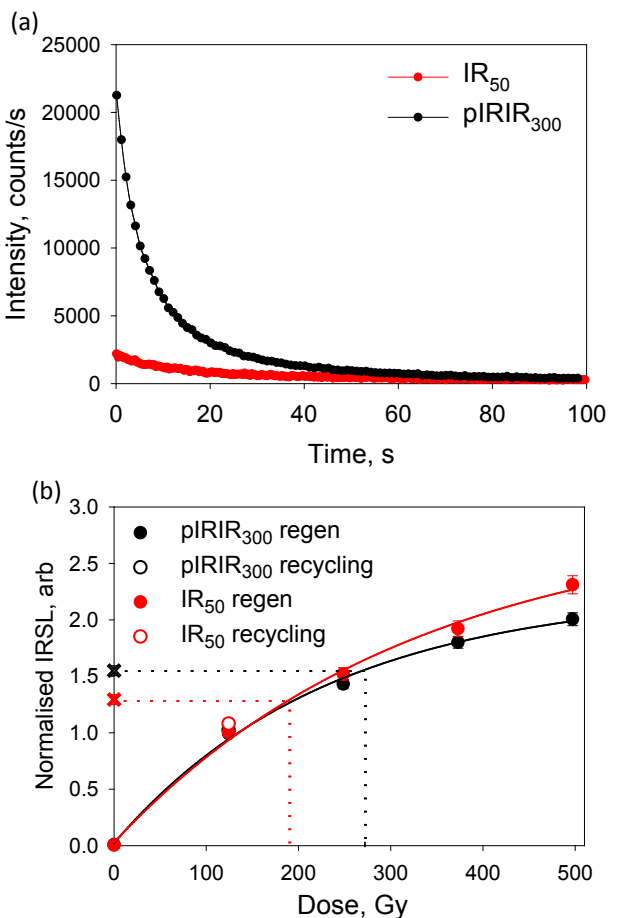


Fig. 6. (a) Decay curves of IRSL signal at 50°C (IR₅₀) and post-IR IRSL (pIRIR₃₀₀) signal at 300°C from one aliquot from AS-TGB-1. (b) Dose response curves for IR₅₀ and pIRIR₃₀₀ signals from the same sample.

ues (**Fig. 7a**) with overdispersions of between 10 and 17%. The pIRIR₃₀₀ ages were calculated to 90 ± 7 , 82 ± 6 , and 101 ± 8 ka for AS-TGB-1, -2, and -4, respectively, which are comparable with that of Aso-4 (86.8–87.3 ka, Aoki, 2008). These data suggest that the pIRIR₃₀₀ signal was not bleached at all at deposition, but probably reset by the last caldera-forming eruption event (Aso-4). This is not surprising because it is thought that the Takuma gravel bed was probably deposited in a very short period of time rather than normal fluvial sediments deposited under a perennial streamflow condition, and pIRIR signals are known to be very difficult to bleach (Buylaert *et al.* 2012). Nevertheless, the three pIRIR₃₀₀ ages from the Takuma gravel bed can be used as maximum age of the deposition of the bed. Since all the three pIRIR₃₀₀ ages are likely to indicate the same resetting event, the weighted mean of the ages was calculated to be 89 ± 3 ka.

It is known that the IR₅₀ signal bleaches faster than a high temperature pIRIR signal (Buylaert *et al.*, 2012). We measured the IR₅₀ signal as a part of the pIRIR₃₀₀ protocol (**Table 3**), but as mentioned above, it was not possible to calculate g-values for each sample and therefore the fading corrected ages were not calculated. In order to investigate whether the IR₅₀ signal had been bleached at deposition, D_e values from a number of small aliquots (using 2.5 mm aliquot size) was measured using an IRSL SAR protocol (**Table 2**) with a preheat at 280°C (60 s). The same preheat temperature as we used in the pIRIR₃₀₀ protocol (340°C) could not be used, because the high preheat temperature reduces the IR₅₀ signal intensity, and the signal is almost undetectable if a small aliquot is used. The dose distribution of IR₅₀ signal (280°C preheat) shown in **Fig. 7b** are not skewed as expected from an incompletely bleached sample. Thus it is likely that the IR₅₀ signal has also not been bleached before the deposition of the Takuma gravel bed. However, it is also possible that there were small portion of grains which had been bleached at the flood event but our multigrain measurements could not detect such grains.

One interesting phenomena was observed from the fading test of the IR₅₀. The g-values were calculated using the same integration limit as we used for the D_e (initial 10 s minus the last 20 s) and then very high fading rates were obtained. It is impossible to correct the anomalous fading accurately with such high fading rates (7–12%). The g-values were also calculated at different integration limits (10–20 s and 20–60 s) and interestingly the values were drastically decreased (**Fig. 8a**). Similar reduction of g-values was reported by previous studies (Thomsen *et al.*, 2008; Novothny *et al.*, 2010) and was also expected from the model of feldspar luminescence production (Jain and Ankjægaard, 2011; Jain *et al.*, 2012). The reduction of g-values is expected to be accompanied by an increasing D_e values towards the latter part of the decay curve. We calculated D_e values for the all three integration limits (**Fig. 8b**), however, the D_e value did not change with the integration limit. We there-

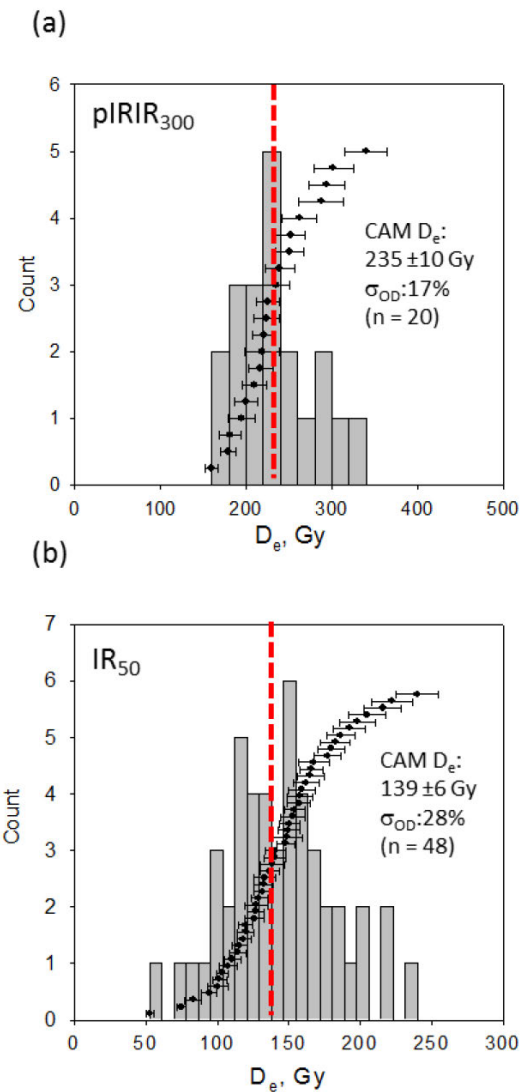


Fig. 7. D_e distributions of (a) pIRIR₃₀₀ signal using medium aliquot and (b) IR₅₀ signal using small aliquots from AS-TGB-1.

fore could not select a g-value for fading correction for the IR₅₀ ages, and it was not possible to calculate fading corrected IR₅₀ ages.

SUMMARY

The pIRIR₂₉₀ ages from loess deposits overlying the Takuma gravel bed suggest a minimum age of the Takuma gravel bed of ~72 ka. The pIRIR₃₀₀ signal from plagioclase showed negligible anomalous fading. However, pIRIR₃₀₀ D_e values showed a tight dose distribution and the age is indistinguishable from the Aso-4 eruption age. The age of the Takuma gravel bed is likely to be constrained between ~72 and 89 ka from the result of this study.

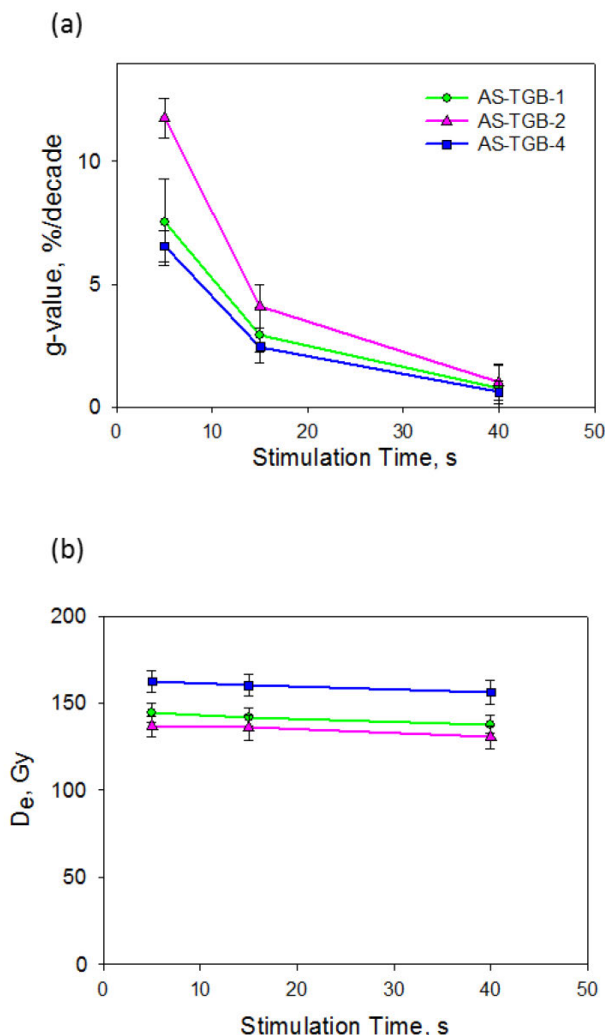


Fig. 8. (a) Variation in g-values of IR₅₀ signal from Takuma gravel bed samples with different signal integration limits. (b) D_e values at corresponding integration limits as in (a).

ACKNOWLEDGEMENTS

The authors thank Dr. Hideo Kubotera and the National Agriculture Research Centre for Kyushu Okinawa Region for permission and logistic support during sampling at the research centre. Jingran Zhang, Sabine Mogwitz, and Sonja Riemenschneider of Leibniz Institute for Applied Geophysics are thanked for their help in sample preparation and the gamma spectrometry measurements. Dr. Reiner Dorhmann of Federal Institute for Geosciences and Natural Resources (BGR) is thanked for the XRD analysis. Funding for this study was provided by the Japanese Ministry of Education, Culture, Sports, Science and Technology (PI: Kyoko S. Kataoka, no. 2074294, Grant-in-Aid for Young Scientists (B) category) and by the Kurita Water and Environment Foundation (PI: Kyoko S. Kataoka, Research Grant Program no. 23343).

REFERENCES

- Aoki K, 2008. Revised age and distribution of ca. 87 ka Aso-4 tephra based on new evidence from the northwest Pacific Ocean. *Quaternary International* 178(1): 100-118, DOI 10.1016/j.quaint.2007.02.005.
- Auclair M, Lamothe M and Huot S, 2003. Measurement of anomalous fading for feldspar IRSL using SAR. *Radiation Measurements* 37(4-5): 487-492, DOI 10.1016/S1350-4487(03)00018-0.
- Buylaert J-P, Jain M, Murray AS, Thomsen KJ, Thiel C and Sohbati R, 2012. A robust method for increasing the age range of feldspar IRSL dating. *Boreas* 41(3): 435-451, DOI 10.1111/j.1502-3885.2012.00248.x.
- Denby PM, Bøtter-Jensen L, Murray AS, Thomsen KJ and Moska P, 2006. Application of pulsed OSL to the separation of the luminescence components from a mixture of quartz/feldspar samples. *Radiation Measurements* 41(7-8): 774-779, DOI 10.1016/j.radmeas.2006.05.017.
- Frechen M, Schweitzer U and Zander A, 1996. Improvements in sample preparation for the fine grain technique. *Ancient TL* 14: 15-17.
- Galbraith RF, Roberts RG, Laslett GM, Yoshida H and Olley JM, 1999. Optical dating of single and multiple grains of quartz from Jinmium rock shelter, Northern Australia: part 1, experimental details and statistical models. *Archaeometry* 41(2): 339-364, DOI 10.1111/j.1475-4754.1999.tb00987.x.
- Guérin G, Mercier N and Adamiec G, 2011. Dose-rate conversion factors: update. *Ancient TL* 29: 5-8.
- Hunter AG, 1998. Intracrustal Controls on the Coexistence of Tholeiitic and Calc-alkaline Magma Series at Aso Volcano, SW Japan. *Journal of Petrology* 39(7): 1255-1284, DOI 10.1093/petroj/39.7.1255.
- Huntley DJ and Lamothe M, 2001. Ubiquity of anomalous fading in K-feldspars and the measurement and correction for it in optical dating. *Canadian Journal of Earth Sciences* 38(7): 1093-1106, DOI 10.1139/e01-013.
- Jain M, Guralnik B and Andersen M, 2012. Stimulated luminescence emission from localized recombination in randomly distributed defects. *Journal of Physics, Condensed Matter* 24(38): 385402, DOI 10.1088/0953-8984/24/38/385402.
- Jain M and Ankjærgaard C, 2011. Towards a non-fading signal in feldspar: Insight into charge transport and tunnelling from time-resolved optically stimulated luminescence. *Radiation Measurements* 46(3): 292-309, DOI 10.1016/j.radmeas.2010.12.004.
- Kataoka KS, 2011. Geomorphic and sedimentary evidence of a gigantic outburst flood from Towada caldera after the 15 ka Towada-Hachinohe ignimbrite eruption, northeast Japan. *Geomorphology* 125(1): 11-26, DOI 10.1016/j.geomorph.2010.08.006.
- Kataoka KS and Miyabuchi Y, 2011. Outflow event from the Aso caldera lake. *2011 PERC Planetary Geology Field Symposium Guidebook for fieldtrip* 37-40.
- Kataoka KS, Urabe A, Manville V and Kajiyama A, 2008. Breakout flood from an ignimbrite-dammed valley after the Numazawako eruption, northeast Japan. *Geological Society of America Bulletin* 120(9-10): 1233-1247, DOI 10.1130/B26159.1.
- Kreuzer S, Schmidt C, DeWitt R and Fuchs M, submitted. The a-value of polymineral fine grain samples measured with the post-IR IRSL protocol. *Radiation Measurements*.
- Lai ZP, Zöller L, Fuchs M and Brückner H, 2008. Alpha efficiency determination for OSL of quartz extracted from Chinese loess. *Radiation Measurements* 43(2-3): 767-770, DOI 10.1016/j.radmeas.2008.01.022.
- Lapp T, Jain M, Ankjærgaard C and Pirtzel L, 2009. Development of pulsed stimulation and Photon Timer attachments to the Risø TL/OSL reader. *Radiation Measurements* 44(5-6): 571-575, DOI 10.1016/j.radmeas.2009.01.012.
- Machida H and Arai F, 2003. Atlas of tephra in and around Japan (revised version). The University of Tokyo Press, 337p (in Japanese).
- Manville V, White JDL, Houghton BF and Wilson CJN, 1999. Paleohydrology and sedimentology of a post-1.8 ka breakout flood from intracaldera Lake Taupo, North Island, New Zealand. *Geological*

- Society of America Bulletin 111(10): 1435-1447, DOI 10.1130/0016-7606(1999)111<1435:PASOAP>2.3.CO;2.
- Mortheikai P, Jain M, Murray AS, Thomsen K and Bøtter-Jensen L, 2008. Fading characteristics of martian analogue materials and the applicability of a correction procedure. *Radiation Measurements* 43(2-6): 672-678, DOI 10.1016/j.radmeas.2008.02.019.
- Novothny A, Frechen M, Horvath E, Krabetzchek M and Tsukamoto S, 2010. Infrared stimulated luminescence and radiofluorescence dating of aeolian sediments from Hungary. *Quaternary Geochronology* 5(2-3): 114-119, DOI 10.1016/j.quageo.2009.05.002.
- Ono K and Watanabe K, 1985. Geological map of Aso Volcano (1:50,000). Geological Map of Volcanoes 4. Geological Survey of Japan (in Japanese with English abstract).
- Ono K, Matsumoto Y, Miyahisa M, Teraoka Y and Kambe N, 1977. Geology of the Taketa district. Geological Survey of Japan, 145p (in Japanese with English abstract).
- Park C and Schmincke H-U, 1997. Lake formation and catastrophic dam burst during the Late Pleistocene Laacher See eruption (Germany). *Naturwissenschaften* 84: 521-525.
- Prescott JR and Hutton JT, 1994. Cosmic ray contributions to dose rates for luminescence and ESR dating: Large depths and long-term time variations. *Radiation Measurements* 23(2-3): 497-500, DOI 10.1016/1350-4487(94)90086-8.
- Sohbati R, Murray AS, Buylaert JP, Ortúñoz M, Cunha PP and Masana E, 2012. Luminescence dating of Pleistocene alluvial sediments affected by the Alhama de Murcia fault (eastern Betics, Spain) – a comparison between OSL, IRSL and post-IR IRSL ages. *Boreas* 41(2): 250-262, DOI 10.1111/j.1502-3885.2011.00230.x.
- Suzuki T, 1995. Origin of so-called volcanic ash soil: thickness distribution in and around central Japan. *Bulletin of the Volcanological Society of Japan* 40: 167-176 (in Japanese with English abstract).
- Thiel C, Buylaert J-P, Murray AS, Terhorst B, Hofer I, Tsukamoto S and Frechen M, 2011a. Luminescence dating of the Stratzing loess profile (Austria) - Testing the potential of an elevated temperature post-IR IRSL protocol. *Quaternary International* 234(1-2): 23-31, DOI 10.1016/j.quaint.2010.05.018.
- Thiel C, Buylaert J-P, Murray AS and Tsukamoto S, 2011b. On the applicability of post-IR IRSL dating to Japanese loess. *Geochronometria* 38(4): 369-378, DOI 10.2478/s13386-011-0043-4.
- Thomsen KJ, Murray AS, Jain M, Bøtter-Jensen L, 2008. Laboratory fading rates of various luminescence signals from feldspar-rich sediment extracts. *Radiation Measurements* 43(9-10): 1474-1486, DOI 10.1016/j.radmeas.2008.06.002.
- Tsukamoto S and Duller GAT, 2008. Anomalous fading of various luminescence signals from terrestrial basaltic samples as Martian analogues. *Radiation Measurements* 43(2-6): 721-725, DOI 10.1016/j.radmeas.2007.10.025.
- Tsukamoto S, Duller GAT, Wintle AG and Muhs D, 2011. Assessing the potential for luminescence dating of basalts. *Quaternary Geochronology* 6(1): 61-70, DOI 10.1016/j.quageo.2010.04.002.
- Tsukamoto S, Duller GAT, Wintle AG and Frechen M, 2010. Optical dating of a Japanese marker tephra using plagioclase. *Quaternary Geochronology* 5(2-3): 274-278, DOI 10.1016/j.quageo.2009.02.002.
- Tsukamoto S, Murray AS, Huot S, Watanuki T, Denby PM and Bøtter-Jensen L, 2007. Luminescence property of volcanic quartz and the use of red isothermal TL for dating tephras. *Radiation Measurements* 42(2): 190-197, DOI 10.1016/j.radmeas.2006.07.008.
- Tsukamoto S, Rink WJ and Watanuki T, 2003. OSL of tephric loess and volcanic quartz in Japan and an alternative procedure for estimating D_{α} from a fast OSL component. *Radiation Measurements* 37(4-5): 459-465, DOI 10.1016/S1350-4487(03)00054-4.
- Watanabe K, 1998. Shin-Kumamoto-Shishi (History of Kumamoto City), 103-108 (in Japanese).
- Watanabe K, Takada H, Okabe R and Nishida A, 1995. Stratigraphic relation between fluvial terrace deposits and widespread tephra beds in the middle reaches of the Shirakawa, Kumamoto Prefecture, Japan. Memoirs of the Faculty of Education, Kumamoto University, 44, 15-22 (in Japanese with English abstract).
- Watanuki T, Murray AS and Tsukamoto S, 2005. Quartz and poly-mineral luminescence dating of Japanese loess over the last 0.6 Ma: comparison with an independent chronology. *Earth and Planetary Science Letters* 240(3-4): 774-789, DOI 10.1016/j.epsl.2005.09.027.
- Wada K, 1987. Minerals formed and mineral formation from volcanic ash by weathering. *Chemical Geology* 60(1-4): 17-28, DOI 10.1016/0009-2541(87)90106-9.
- Waythomas CF, Walder JS, McGimsey RG and Neal CA, 1996. A catastrophic flood caused by drainage of a caldera lake at Aniakchak Volcano, Alaska, and implications for volcanic hazards assessment. *Geological Society of America Bulletin* 108(7): 861-871, DOI 10.1130/0016-7606(1996)108<0861:ACFCBD>2.3.CO;2.